Effect of Nanorod Alignment on Flux Pinning State in $BaHfO_3$ Doped $SmBa_2Cu_3O_y$ Films

Y. Tsuchiya, S. Miura, Q. Xu, Y. Ichino, Y. Yutaka, S. Awaji, and K. Watanabe

***Abstract*—The effect of the microstructure on the flux pinning state in $BaHfO_3$(BHO) nanorods doped $SmBa_2Cu_3O_y$(SmBCO) films was investigated using high field magnets with a rotator stage. A films with aligned nanorods showed the strong flux pining along *c*-axis, which disappears at high magnetic fields. This behavior corresponds to the existence of the Bose glass state in the film which is also supported by the behaviors of the activation energy and the critical exponent of the liquid-glass transition estimated from the transport properties. Moreover, the field dependences of the flux pinning force are explained by the flux pinning models for the correlated nanorods and the random pinning centers in the films with the aligned and the firework nanorods structures. The strong relationship is confirmed between the structure of the nanorods and the pinning properties in the BHO doped SmBCO films.**

***Index Terms*— High temperature superconductors, Superconducting Films, Flux pinning, Critical current density, Nanostructured materials.**

I. Introduction

FLUX pinning is the key to enhance the current capacity of the high temperature superconducting wires and tapes for the high temperature and high magnetic field applications because the critical current rapidly decreases at high temperatures due to thermally fluctuated vortex motion [1]-[4]. To overcome the problem of the operation at high temperatures, it is necessary to introduce pinning centers intentionally into the wires and tapes, which is known as artificial pining centers (APCs) [5]-[7]. Among the high temperature superconductors, REBa$_2$Cu$_3$O$_y$ (REBCO, RE = rare earth elements and Y) tapes are the strong candidate for the applications at high temperatures and the high magnetic field at present. To enhance the flux pinning at high temperatures in REBCO tapes, self-organized nanorods have been enthusiastically studied over ten years. Especially, BaMO$_3$ (BMO) materials forms narrow nanorods and extremely enhance flux pinning in the PLD or the CVD processed REBCO tapes [8]-[10]. According to the material researches, M = Sn, Hf, Zr are the elements to form the nanorods. For further improvements, it is necessary to discuss the vortex pinning mechanisms and the microstructure from the physical view point. The shape of the BMO nanorods depends on the growth conditions especially on temperature [11]-[14]. In recent years, our group developed a growth technique to control the shape of the nanorod, where the REBCO seed layer is deposited at usual temperature before fabrication of the nanorod doped REBCO film at relatively low temperature to extend the growth temperature range without appearance of the impurity such as *a*-axis oriented grains. We call the 2 step fabrication method as the "low temperature growth (LTG)" technique. According to the microstructure analysis, nanorods tend to become narrow, discontinuous, and inclined with the LTG technique. In this work, we investigate the effect of the nanorod alignments on the vortex pinning state in $SmBa_2Cu_3O_y$ (SmBCO) films with the $BaHfO_3$ (BHO) nanorods by controlling the nanorod alignment using the LTG technique.

II. Experimental Method

SmBCO films with BHO nanords were fabricated on $LaAlO_3$ (001) substrates using the alternating-target pulse laser deposition method with KrF excimer laser (248 nm wavelength) [12]-[14]. The targets were $SmBa_2Cu_3O_y$ and $BaHfO_3$. The LTG technique was adopted to incline the nanorods. The ~50 nm thick SmBCO seed layer was firstly deposited at 840 °C and then the ~300 nm thick BHO doped SmBCO upper layer was deposited at 750 °C with the laser pulse frequency of 10 Hz and with the laser pulse energies of 52 and 53 mJ. The BHO content is fixed as 1.6vol.%. Figure 1 shows TEM images of two samples with aligned and inclined nanorods with the smaller and the larger energies of the laser pulses, respectively. We put names of the samples as "Aligned" and "Firework" films. According to the resistivity measurement, T_c of the Aligned and the Firework films are 90.3 K and 91.9 K, respectively. In the Aligned film, nanorods distributes uniformly as shown in Fig. 1(a) and the nanorods are aligned as shown in Fig. 1(b). The nanorods alignment is quantitatively analyzed in the following part. On the contrary in the Firework film, the nanorods are located radially as shown in Fig. 1(c) and are inclined against the *c*-axis of the SmBCO matrix as shown in Fig. 1(d). The nanorod density is calculated as 1000 μm^{-2} in the Aligned film as 2 T, but not for the Firework film because of the inhomogeneous distribution of the nanorods. Transport properties including the critical current density J_c and the resistivity ρ were measured in high magnetic fields at wide range of temperatures using the 20 T superconducting magnets at HFLSM, IMR, Tohoku Univ. The resistivity is measured

This work was supported by a Grant-in-Aid for Scientific Research from the Japan Society for the Promotion of Science (JSPS) (No. 25246032, 15H04252, 15K14301, 15K14302,16K20898), JST-ALCA, NU-AIST alliance project, The Murata Science Foundation, Research Foundation for the Electrotechnology of Chubu, and co-research program with Tohoku Univ. (16H0009)).

Y. Tsuchiya, S. Miura, Q. Xu, Y. Ichino, Y. Yutaka are with Nagoya University. Nagoya 464-8603, Japan. (e-mail: tsuchiya@nuee.nagoya-u.ac.jp)

S. Awaji, and K. Watanabe are with High Field Laboratory for Superconducting Materials, Institute for Materials Research, Tohoku Univeristy, Sendai 980-8577, Japan.

with the fixed current density of 10 A/cm^2 and J_c has the fixed electric field criterion of 1 μV/cm and the irreversible magnetic field B_{irr} is defined with a criterion of the J_c of 10 A/cm^2. B_{irr} is estimated with the same criterion of J_c based on interpolation between the measured points of different field and temperatures.

Fig. 1 Here

III. Results and Discussion

First, the TEM images are analyzed with distribution of the inclined angle against *c*-axis of the SmBCO matrix. Figure 2 shows the histogram of the nanorods angle from *c*-axis of the films. The distribution is apparently wide for the Firework films. According to the planer view of the TEM images as shown in Fig.1(a) and 1(c), the nanorods looks like circle and oval in the Aligned and Firework films, respectively, because of the angle between the nanorods and the in-plane. The angle distribution is fitted with the Gaussian curves and the characteristic angle distributions are calculated. The Aligned and the Firework films have the characteristic angle of 8.4° and 24.1°, respectively, which are relatively large values compared with the ones for the conventional PLD method [12]-[14]. The angle distribution of the nanorods is related with the perpendicular growth rate of the REBCO matrix compared with the BMO nanorods [15].

Fig. 2 Here

Figure 3(a) shows field dependences of J_c at 77 K in the Firework and the Aligned films under perpendicular magnetic fields. The Aligned film has a plateau of J_c at low magnetic fields and a shoulder around 2 T. This behavior of J_c is typically observed in the REBCO films with the *c*-axis correlated pinning centers [12], [13]. The shoulder is understood as the maximum field where the pinning center is saturated and effective so called as the matching field [12], [16], [17]. According to the nanorod density of the TEM images in Fig. 1, the matching field B_Φ is calculated as 2 T, where it is calculated as $B_\Phi = n*\Phi_0$, where Φ_0 is the quantized flux in superconductors as $2.07*10^{-15}$ Tm^2. On the contrary, the Firework films have no shoulder possibly because of the not correlated pinning centers. We will discuss the reason why the Firework film has no shoulder later in this paper. In high fields over 4 T, J_c in the Firework film is larger than one in the Aligned film possibly due to the difference of T_c in the films.

Figure 3(b) shows the field angular dependence of J_c at 77 K and various magnetic fields of 1, 3, and 5 T. The angle is defined as angles from the *c*-axis of the films. The curves have peaks at 0° for each fields and samples. The peaks are apparently wide in the Firework films compared with the Aligned films. The angle distribution of the nanorod matches well with the peak width at low magnetic fields. This results support the correlation between the nanorods orientation and the anisotropy of J_c, especially about the peak structure. The peaks disappear at high magnetic fields and the similar curve appears for both the films. It indicates that the nanorods becomes less effective with increasing the field. This behavior is explained by the transition of the flux pinning state from the single vortex pinning to the collective vortex pinning state where vortices support each other against the force from the flowing current [18]-[20]. It indicates that the peak width becomes wider with increasing the magnetic field at low fields because the contribution of the two kinds flux pinning changes. We note that the peak structure is tunable with the different nanorod distribution by changing the deposition conditions. For example, the Firework film has a very flat angular dependence at 77 K, 3 T. The effect of the nanorods remains even around or above the irreversible fields. These behaviors are understood as follows. The flux pinning in the nanorods doped the REBCO films divided into two components; the *c*-axis correlated pinning and the random pinning. The correlated pinning is caused by the nanorods, the twin boundaries, the grain boundaries, and the spiral dislocation. On the other hand, the random pinning is realized by the lattice dislocation, the oxygen vacancy, or other defects such as the precipitants. According to our transport results and the earlier studies, the correlated pinning is dominant at low magnetic field less than the matching field and the higher fields around or even above the irreversible fields. On the other hand, the random pinning is dominant at the mid fields. To confirm our speculation, we analyze the resistive properties to determine the flux pinning state.

Fig. 3 Here

Figure 4 shows field dependences of the activation energy and the critical exponents of the vortex liquid-glass transition. The activation energy U_0 is the energy required to shake vortices off from the nanorods or other pinning centers. The inset figure in Fig. 4(a) shows logarithm of the resistivity ρ vs the inversed temperature. This curve is called as the Arrhenius plot which is generally used for the thermally activated phenomena. The flux flow just above T_c is dominated by the thermally activated flux flow [1]-[4]. Therefore, U_0 is estimated from the linear fitting results as shown in the inset figure of Fig. 4(a). As results, field dependences of U_0 are shown as the main panel of the Fig. 4(a). U_0 monotonically decreases with increasing magnetic fields. They have a shoulder structure near $B_\Phi \sim 2$ T. This is unique behavior of U_0 with a plateau structure and the sharp shoulder in the Aligned films. This indicates that the single vortex pinning state is realized in the field range below the shoulder field because U_0 should be held at the same value in the single vortex pinning state [19], [21]. This matching behavior in U_0 is more apparent than in J_c with the smooth shoulder around the matching field. On the other hand in the Fireworks film, a vague transition from the plateau to the slope appears. It indicates the distribution of the nanorod density in the films as show in Fig. 1(d). In higher magnetic field, U_0 is proportional to B^{-1} in each film. This behavior is an evidence of the collective vortex pinning [19], [21]. These results suggest that a part of vortices are located at the interstitial area out of the nanorods and the motion of the interstitial vortices or the bundle motion of vortices are the key to determine the flux pinning force above B_Φ in the Aligned films or above small fields in the Firework film.

Fig. 4 Here

The critical exponent of the liquid-glass state transition of vortices s is estimated from the linear fitting for the inverse of the temperature derivative of the logarithm resistivity vs temperature near the glass temperature [3], [22]-[26]. The fitting is shown in the inset figure in Fig.4(b). From the fitting results, in addition to s, the glass-liquid transition temperature of the vortex T_g is calculated as a extrapolated temperature. The inset figure is a typical fitting result for the Aligned film. Adopting the same fitting method for the other conditions and the Firework film, the field dependences of s in both films are shown in the main panel in Fig. 4(b). Among the all field, s in the Firework film is larger than the one in the Aligned film. s in the Firework is almost constant near 8, on the other hand, s in the Aligned film monotonically increases for larger fields and is saturated at around 1 T as a half of B_Φ. The small s value as 4-6 at low fields indicates the existence of the Bose glass state where the vortices are individually trapped in the correlated pinning centers [19], [22], [23]. In the Bose glass state, the flux pinning by the nanorods becomes strong and the ideal matching effect is expected to appear.

Figure 5 show normalized F_p curves as a function of normalized magnetic fields in each sample. At low temperatures, F_p is normalized by its maximum value. The magnetic field is also normalized by the peak field B_{peak} where F_p becomes the maximum. On the other hand at high temperatures, two peaks appear possibly due to the many rods pinning or the delocalization of the vortex [19], [27], [28], [33] . The peak fields B_{peak} are estimated with 3 order polynomial fittings even when the two peaks of F_p appear. Finally, F_p is normalized at the higher peak fields B_{peak} at each temperature. As results, the F_p curves in the Aligned film have the linear field dependences at the field less than the magnetic field at low temperature less than 80 K. This behavior is explained by the individual flux pinning by the nanorods in the Aligned film and F_p should be proportional to B. On the other hand, the F_p curves in the Firework films have round-shaped at all temperature. To speculate the origin of the flux pinning in the Firework film, the typical F_p curve is plotted as a dashed line according to the collective pinning state with an equation of $F_p \propto (B/B_{irr})^{-0.5}(1-B/B_{irr})^2$ by randomly distributed pinning centers [21], [29]. It is clear that the F_p curves at the low temperatures in the Firework film matches well with the typical curve. According to the results, the flux pinning state in the films are quite different; the individual vortex pinning state with the Bose glass state at less than B_Φ in the Aligned films, and the collective vortex pinning state over wide temperature range in the Firework film [30], [31].

Fig. 5 Here

To summarize the transport measurements, phase diagrams as functions of magnetic field and temperature are plotted with the irreversible line [32], the glass-liquid transition line, and the peak field of F_p as shown in Fig. 6. As explained previously, the irreversible magnetic field B_{irr} is defined as the J_c criterion of 10 A/cm^2. The glass transition field B_g is estimated based the extrapolation of the critical exponent fitting. The peak field of F_p is estimated from the polynomial fitting of the field dependences of peak F_p. It is apparent that the peak field B_{peak} has a plateau at the low temperatures due to the matching effect where the flux pinning by the c-axis correlated nanorods becomes most dominant in the Aligned films. On the other hand, B_{peak} in the Firework films monotonically increases with decreasing the temperature. This behavior is observed in the films with the randomly distributed pinning centers such as the pure REBCO films, where B_{peak} is scaled by B_{irr}. According to the systematic experimental results on the flux pinning properties with different nanorod structures, we confirmed a strong relationship between the shape of the nanorods and the flux pinning landscapes. With the correlated pinning centers such as the straight nanorods in Fig. 1(b), the peak field B_{peak} is saturated at the low temperature, and the Bose glass state would be realized. On the contrary with the randomly distributed or the non-correlated nanorods, the peak field B_{peak} monotonically increases at low temperatures because B_{peak} is scaled with the irreversible field B_{irr}. Based on this analysis, the microstructure of the nanorods in the films would be speculated without TEM imaging.

Next, the high temperature range is shown in Fig. 6(b) with the normalized temperature with T_c. The Aligned film has a shoulder in the irreversibility line and the glass-liquid transition line near the matching field of 2 T. On the other hand, the Firework films has a smooth curve for both the lines. The irreversibility line should show shoulders in the Bose glass phase [12], [32], [33].

Fig.6 Here

IV. Conclusion

The influence of the nanorod microstructure on the flux pinning state in BHO doped SmBCO films is investigated using high field magnets with the rotator stage. The inclined nanorods are realized using the low temperature growth technique. The alignment of the nanorods are controlled with energy of the laser pulses. The films with aligned nanorods show the strong flux pining along the c-axis, which disappears at high magnetic fields. This behavior is supported by the existence of the Bose glass phase in the film according to the discussion on the activation energy and the critical exponent measured by the transport properties. On the contrary, the films with firework nanorods show weak correlated pinning along c-axis such as the disappearance of the Bose glass state or the weak matching effect. Moreover, the temperature dependence of the peak field of the flux pinning force is explained by the flux pinning model for the correlated nanorods and the random pinning model for the films with the aligned and the firework nanorods structures. We confirmed the strong relationship between the microstructure of the BMO nanorods and the flux pinning landscapes according to the transport properties in the BMO doped REBCO films.

ACKNOWLEDGMENT

We thank Mr. Shun Ito at IMR, Tohoku Univ. for his contribution to take TEM images.

REFERENCES

[1] D. R. Nelson, "Vortex Entanglement in High-T_c Superconductors," Phys. Rev. Lett., vol. 60, no. 19, pp. 1973–1976, May 1988.
[2] A. Houghton, R. A. Pelcovits, and A. Sudbø, "Flux lattice melting in high-T_c superconductors," Phys. Rev. B, vol. 40, no. 10, pp. 6763–6770, Oct. 1989.
[3] M. P. A. Fisher, "Vortex-glass superconductivity: A possible new phase in bulk high-T_c oxides," Phys. Rev. Lett., vol. 62, no. 12, pp. 1415–1418, 1989.
[4] D. S. Fisher, M. P. A. Fisher, and D. A. Huse, "Thermal fluctuations, quenched disorder, phase transitions, and transport in type-II superconductors," Phys. Rev., vol. 43, no. 1, pp. 130–159, 1991.
[5] J. L. MacManus-Driscoll, S. R. Foltyn, Q. X. Jia, H. Wang, A. Serquis, L. Civale, B. Maiorov, M. E. Hawley, M. P. Maley, and D. E. Peterson, "Strongly enhanced current densities in superconducting coated conductors of $YBa_2Cu_3O_{7-x}$ + $BaZrO_3$," Nat Mater, vol. 3, no. 7, pp. 439–443, May 2004.
[6] B. Maiorov, S. A. Baily, H. Zhou, O. Ugurlu, J. A. Kennison, P. C. Dowden, T. G. Holesinger, S. R. Foltyn, and L. Civale, "Synergetic combination of different types of defect to optimize pinning landscape using $BaZrO_3$-doped $YBa_2Cu_3O_7$," Nat Mater, vol. 8, no. 5, pp. 398–404, Apr. 2009.
[7] J. Gutiérrez, A. Llordés, J. Gázquez, M. Gibert, N. Romà, S. Ricart, A. Pomar, F. Sandiumenge, N. Mestres, T. Puig, and X. Obradors, "Strong isotropic flux pinning in solution-derived $YBa_2Cu_3O_{7-x}$ nanocomposite superconductor films," Nat Mater, vol. 6, no. 5, pp. 367–373, Apr. 2007.
[8] H. Tobita, K. Notoh, K. Higashikawa, M. Inoue, T. Kiss, T. Kato, T. Hirayama, M. Yoshizumi, T. Izumi, and Y. Shiohara, "Fabrication of $BaHfO_3$ doped $GdBa_2Cu_3O_{7-\delta}$ coated conductors with the high I_c of 85 A/cm-w under 3 T at liquid nitrogen temperature (77 K)," Supercond. Sci. Technol., vol. 25, no. 6, p. 062002, May 2012.
[9] A. Tsuruta, Y. Yoshida, Y. Ichino, A. Ichinose, K. Matsumoto, and S. Awaji, "The influence of the geometric characteristics of nanorods on the flux pinning in high-performance BaMO$_3$-doped $SmBa_2Cu_3O_y$ films (M = Hf, Sn)," Supercond. Sci. Technol., vol. 27, no. 6, p. 065001, Apr. 2014.
[10] A. Tsuruta, Y. Yoshida, Y. Ichino, A. Ichinose, K. Matsumoto, and S. Awaji, "Flux Pinning Properties at Low Temperatures in SmBaCuO Films," IEEE Trans. Appl. Supercond., vol. 23, no. 3, pp. 8001104–8001104, Jun. 2013.
[11] Y. Yoshida, K. Matsumoto, M. Miura, Y. Takai, A. Ichinose, S. Horii, and M. Mukaida, "High-Critical-Current-Density $SmBa_2Cu_3O_{7-x}$ Films Induced by Surface Nanoparticle," Jpn. J. Appl. Phys., vol. 44, no. 18, pp. L546–L548, Apr. 2005.
[12] S. Miura, Y. Yoshida, Y. Ichino, A. Tsuruta, K. Matsumoto, A. Ichinose, and S. Awaji, "Flux pinning properties and microstructures of a $SmBa_2Cu_3O_y$ film with high number density of $BaHfO_3$ nanorods deposited by using low-temperature growth technique," Jpn. J. Appl. Phys., vol. 53, no. 9, p. 090304, Aug. 2014.
[13] S. Miura, Y. Yoshida, Y. Ichino, Y. Doki, A. Ibi, T. Izumi, and T. Kato, "Flux Pinning Properties in $BaHfO_3$-Doped $SmBa_2Cu_3O_y$ Films on Metallic Substrates Fabricated With Low Temperature Growth," IEEE Trans. Appl. Supercond., vol. 26, no. 4, pp. 1–5, Jan. 2016.
[14] S. Miura, Y. Yoshida, Y. Ichino, Q. Xu, K. Matsumoto, A. Ichinose, and S. Awaji, "Improvement in J_c performance below liquid nitrogen temperature for $SmBa_2Cu_3O_y$ superconducting films with $BaHfO_3$ nano-rods controlled by low-temperature growth," APL Mater., vol. 4, no. 1, pp. 016102–9, Jan. 2016.
[15]M. Mukaida, A. Ichinose, P. Mele, K. Mtsumoto, and S. Horii, "An Explanation for Bends of 1-Dimensional Nanorods," *Physics Procedia*, 2012.
[16] T. Horide, K. Matsumoto, A. Ichinose, M. Mukaida, Y. Yoshida, and S. Horii, "Matching field effect of the vortices in $GdBa_2Cu_3O_{7-\delta}$ thin film with gold nanorods," Supercond. Sci. Technol., vol. 20, no. 4, pp. 303–306, Feb. 2007.
[17] L. Krusin-Elbaum, L. Civale, J. R. Thompson, and C. Feild, "Accommodation of vortices to columnar defects: Evidence for large entropic reduction of vortex localization," Phys. Rev. B, vol. 53, no. 17, pp. 11744–11750, May 1996.
[18] L. Civale, "Vortex pinning and creep in high-temperature superconductors with columnar defects," Supercond. Sci. Technol., vol. 10, no. 7, pp. A11–A28, Jul. 1997.
[19] G. Blatter, V. B. Geshkenbein, A. I. Larkin, and V. M. Vinokur, "Vortices in high-temperature superconductors," Rev. Mod. Phys., vol. 66, no. 4, pp. 1125–1388, Oct. 1994.
[20] L. Civale, B. Maiorov, A. Serquis, and J. O. Willis, "Angular-dependent vortex pinning mechanisms in $YBa_2Cu_3O_7$ coated conductors and thin films," Appl. Phys. Lett., vol. 84, no. 12, p. 2121, 2004.
[21] B. Dam, J. M. Huijbregtse, and F. C. Klaassen, "Origin of high critical currents in $YBa_2Cu_3O_{7-\delta}$ superconducting thin films," Nature, 1999.
[22] D. R. Nelson and V. M. Vinokur, "Boson localization and pinning by correlated disorder in high-temperature superconductors," Phys. Rev. Lett., vol. 68, no. 15, pp. 2398–2401, Apr. 1992.
[23] D. R. Nelson and V. M. Vinokur, "Boson localization and correlated pinning of superconducting vortex arrays," Phys. Rev. B, vol. 48, no. 17, pp. 13060–13097, 1993.
[24] T. Hwa, P. Le Doussal, D. R. Nelson, and V. M. Vinokur, "Flux pinning and forced vortex entanglement by splayed columnar defects," Phys. Rev. Lett., vol. 71, no. 21, pp. 3545–3548, Nov. 1993.
[25] S. Awaji, M. Namba, K. Watanabe, M. Miura, Y. Yoshida, Y. Takai, and K. Matsumoto, "c-axis correlated pinning behavior near the irreversibility fields," Appl. Phys. Lett., vol. 90, no. 12, p. 122501, 2007.
[26] S. Awaji, N. Isono, K. Watanabe, M. Murakami, M. Muralidhar, N. Koshizuka, and K. Noto, "Bose glass state in bulk (Nd,Eu,Gd)$Ba_2Cu_3O_x$ with a high irreversibility field," Phys. Rev. B, vol. 69, no. 21, p. 214522, Jun. 2004.
[27] L. Miu, P. Wagner, A. Hadish, F. Hillmer, H. Adrian, J. Wiesner, and G. Wirth, "Bose-glass behavior of the vortex system in epitaxial $Bi_2Sr_2CaCu_2O_{8+\delta}$ films with columnar defects," Phys. Rev. B, vol. 51, no. 6, pp. 3953–3956, Feb. 1995.
[28] L. Miu, P. Mele, A. Crisan, A. Ionescu, and D. Miu, "Evolution of vortex dynamics in $YBa_2Cu_3O_7$ films with

nanorods by adding nanoparticles," Physica C: Superconductivity and its applications, vol. 500, no. C, pp. 40–43, May 2014.
[29] F. C. Klaassen, G. Doornbos, and J. M. Huijbregtse, "Vortex pinning by natural linear defects in thin films of $YBa_2Cu_3O_{7-\delta}$" Phys. Rev. B, vol. 64, no. 18, p. 184523, 2001.
[30] A. Mazilu, H. Safar, M. Maley, J. Coulter, L. Bulaevskii, and S. Foltyn, "Vortex dynamics of heavy-ion-irradiated $YBa_2Cu_3O_{7-\delta}$: Experimental evidence for a reduced vortex mobility at the matching field," *Phys. Rev. B*, vol. 58, no. 14, pp. R8909–R8912, Oct. 1998.
[31] Fuchs, K. Nenkov, and G. Krabbes, "Strongly enhanced irreversibility fields and Bose-glass behaviour in bulk YBCO with discontinuous columnar irradiation defects," Supercond. Sci. Tech., vol. 20, no. 9, S197-S204, 2007.
[32] M. Konczykowski, F. Rullier-Albenque, and E. R. Yacoby, "Effect of 5.3-GeV Pb-ion irradiation on irreversible magnetization in Y-Ba-Cu-O crystals," Phys. Rev. B, vol. 44, no. 13, pp. 7167–7170, 1991.
[33] Y. Tsuchiya, S. Awaji, K. Watanabe, S. Miura, Y. Ichino, Y. Yoshida, and K. Matsumoto, "Delocalization of Vortex in $SmBa_2Cu_3O_{7-d}$ Superconducting Films with $BaHfO_3$ Nano-rods," Journal of Applied Physics, vol. 120, no. 10, p. 103902, Sep. 2016.

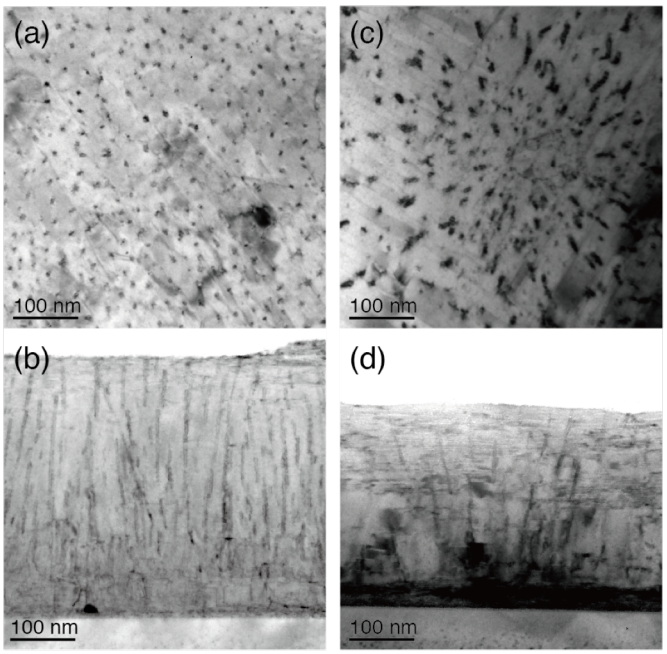

Fig. 1. TEM images for plan-view and elevetion-view in (a), (b) the Aligned and (c), (d) the Firework films.

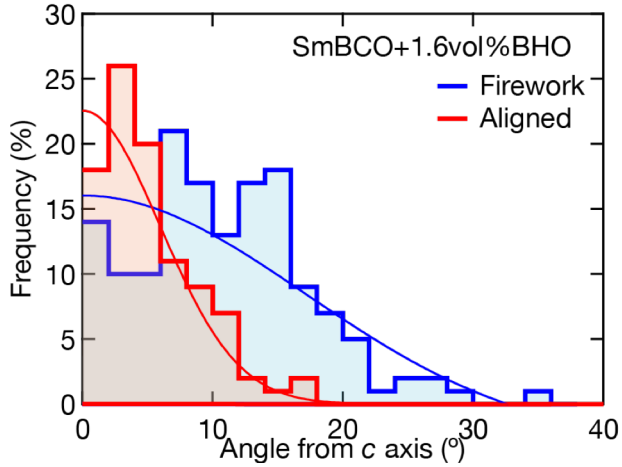

Fig. 2. Population histgram of the nanorod angle from the *c*-axis of the SmBCO matrix in the Aligned and Firework films. The thin lines are Gaussian fitting lines for both the films.

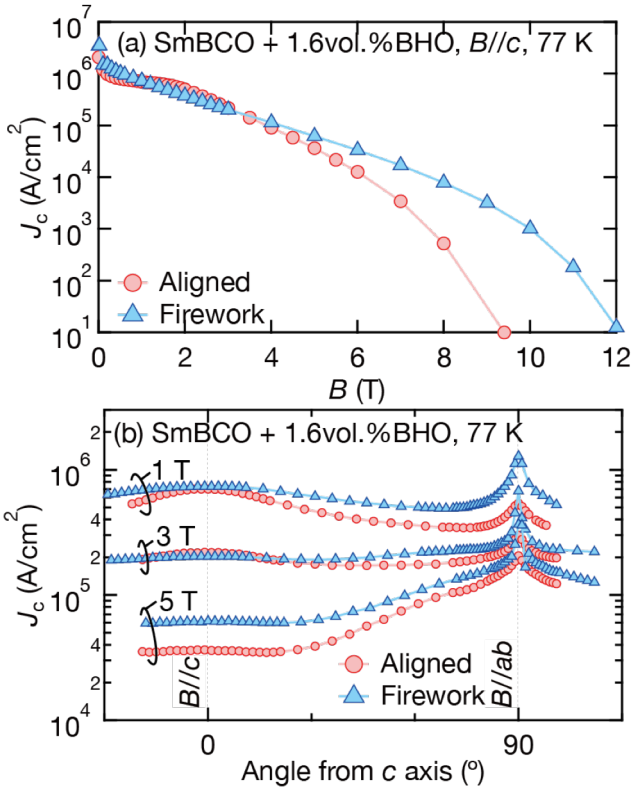

Fig. 3. (a) Field dependences of the critical current density J_c in the Aligned and the Firework films with the perpendicular field at 77 K. (b) Field angular dependences of J_c in each film at 77 K, 1, 3, and 5 T.

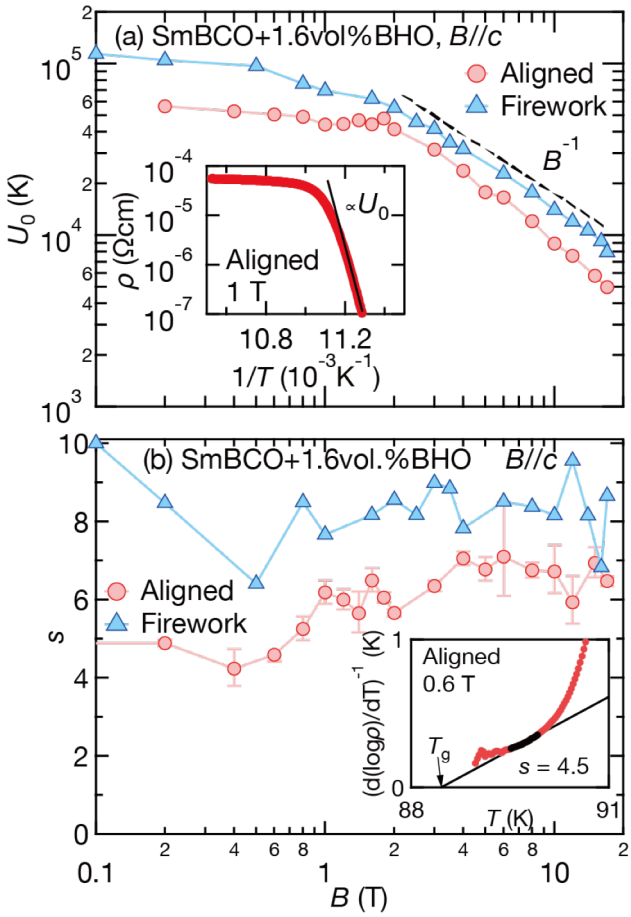

Fig. 4. Field dependences of (a) the activation energy U_0 of the vortex at thermally activated flux flow state just above T_c and (b) the critical exponent s close to the liquid glass transition temperatures in the Aligned and the Firework films. Inset shows the typical fitting results to estimate the activation eneryg and the critical exponent.

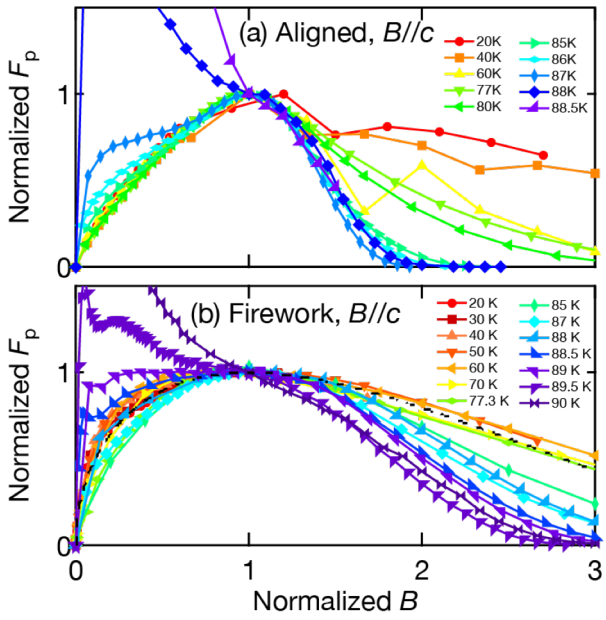

Fig. 5. Normalized magneic field dependences of the normalized flux pinnining force density F_p in (a) Aligned and (b) Firework films at various temperatures with the perpendicular magnetic field. Typical fitting results for the REBCO films are plotted as the dotted line.

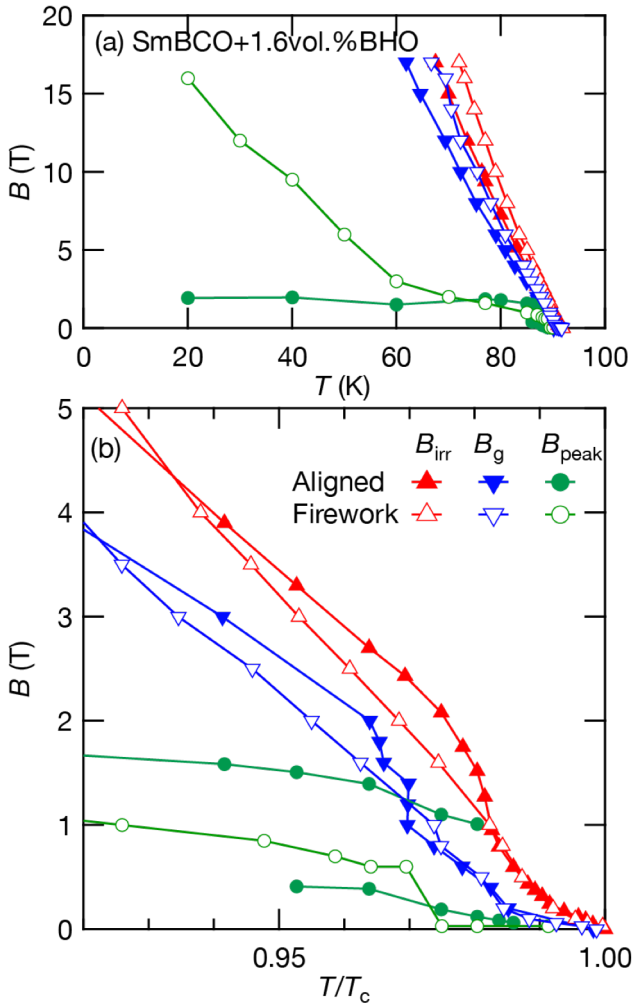

Fig. 6. Temperature dependences of the irreversible field B_{irr} (up triangle), the glass transition temperature T_g (down triangle), and the peak field of the flux pinning force density B_{peak} (circles) in the Aligned (filled) and the Firework (blank) films.